IMPACT/CONTACT OF ELASTIC BODY ON A MOVING FOUNDATION[*]

C. M. Murea[†]

Dedicated to Dr. Dan Tiba on the occasion of his 70th anniversary

Abstract

We study numerically the dynamic impact/contact of an elastic body on a moving foundation using the mid-point algorithm. Stability results are presented when foundation is decreasing. Numerical simulations on two-dimensional problems are included and we show that the energy is absorbed in the case of decreasing foundation compared to the fixed one.

MSC: 74H15, 74S05, 65M12

keywords: dynamic elasticity, frictionless contact, numerical methods, stability

1 Introduction

Several numerical methods have been developed for elastodynamic contact problem, see the textbook [7], [9], [17] or the survey papers [5], [8]. The contact constraint can be treated using: Lagrange multiplier, augmented Lagrangian, penalty methods, etc. We add also the Nitsche based methods [1], [2]. Updated Lagrangian methods for elasticity with contact are described in [18] and [11].

The contact problem can be modeled by variational inequalities. We mention here the textbooks of Dan Tiba on this topic [16], [14] and some applications to contact mechanics [12], [13].

In this paper, we study the mid-point algorithm for the dynamic impact/contact of an elastic body on a moving foundation. In Section 3, stability results are presented. Numerical experiments are included in Section 4 and we show that the energy is absorbed in the case of decreasing foundation compared to the fixed one.

2 Contact without friction in dynamic linear elasticity

We denote by $\Omega_0 \subset \mathbb{R}^2$ the undeformed structure domain. We assume that it has Lipschitz boundary $\partial\Omega_0 = \overline{\Gamma}_D \cup \overline{\Gamma}_N \cup \overline{\Gamma}_C$, where Γ_D, Γ_N and Γ_C are relatively open subsets, mutually disjoint. The structure is elastic and its displacement is denoted by $\mathbf{u} = (u_1, u_2) : \overline{\Omega}_0 \times [0, T] \to \mathbb{R}^2$, where $T > 0$. After deformation, a point $\mathbf{X} = (X_1, X_2) \in \Omega_0$ will occupy the position $\mathbf{x} = \varphi_t(\mathbf{X}) = \mathbf{X} + \mathbf{u}(\mathbf{X}, t)$ in the structure domain at time instant t denoted by $\Omega_t = \varphi_t(\Omega_0)$.

Let $\psi_t \in \mathcal{C}^1(\mathbb{R})$ be a function describing the foundation at time instant t. Its graph will be denoted by

$$graph(\psi_t) = \left\{ \mathbf{X} = (X_1, X_2) \in \mathbb{R}^2; \ X_2 = \psi_t(X_1) \right\}$$

and its epigraph by

$$epi(\psi_t) = \left\{ \mathbf{X} = (X_1, X_2) \in \mathbb{R}^2; \ X_2 \geq \psi_t(X_1) \right\}.$$

We assume that the structure is governed by the linear elasticity equation. The stress tensor is $\sigma(\mathbf{u}) = \lambda(\nabla \cdot \mathbf{u})\mathbf{I} + 2\mu\epsilon(\mathbf{u})$, where $\lambda, \mu > 0$ are the Lamé coefficients, $\epsilon(\mathbf{u}) = \frac{1}{2}(\nabla\mathbf{u} + (\nabla\mathbf{u})^T)$ and $\mathbf{I}$ is the unit matrix.

The problem is to find the structure displacement $\mathbf{u} : \overline{\Omega}_0 \times [0, T] \to \mathbb{R}^2$,

such that:

$$\rho\frac{\partial^2 \mathbf{u}}{\partial t^2} - \nabla \cdot \sigma\left(\mathbf{u}\right) \;=\; \mathbf{f}, \quad \text{in } \Omega_0 \times]0, T[\tag{1}$$

$$\mathbf{u} \;=\; 0, \quad \text{on } \Gamma_D \times]0, T[\tag{2}$$

$$\sigma\left(\mathbf{u}\right)\mathbf{n} \;=\; 0, \quad \text{on } \Gamma_N \times]0, T[\tag{3}$$

$$\varphi_t(\Gamma_C) \;\subset\; epi(\psi_t), \quad t \in]0, T[\tag{4}$$

$$\sigma\left(\mathbf{u}\right)\mathbf{n} \;=\; 0, \text{ on } \{\mathbf{X} \in \Gamma_C; \; \varphi_t(\mathbf{X}) \notin graph(\psi_t)\}, \; t \in]0, T[\tag{5}$$

$$\sigma\left(\mathbf{u}\right)(\mathbf{X}, t)\mathbf{n}(\mathbf{X}) \;=\; -\alpha(\mathbf{X}, t)\mathbf{n}(\mathbf{X}), \quad \alpha(\mathbf{X}, t) \geq 0,$$
$$\text{on } \{\mathbf{X} \in \Gamma_C; \; \varphi_t(\mathbf{X}) \in graph(\psi_t)\}, \; t \in]0, T[\tag{6}$$

$$\mathbf{u}(\mathbf{X}, 0) \;=\; \mathbf{u}_0(\mathbf{X}), \quad \mathbf{X} \in \Omega_0 \tag{7}$$

$$\frac{\partial \mathbf{u}}{\partial t}(\mathbf{X}, 0) \;=\; \mathbf{u}_1(\mathbf{X}), \quad \mathbf{X} \in \Omega_0 \tag{8}$$

where $\mathbf{f} : \overline{\Omega}_0 \times [0, T] \to \mathbb{R}^2$ are the applied volume forces, $\mathbf{n}$ is the unit outward vector normal to $\partial\Omega_0$, $\mathbf{u}_0$ is the initial displacement and $\mathbf{u}_1$ is the initial velocity. Of course, the solution $\mathbf{u}$ have to be smooth enough, such that the system (1)-(8) has sense.

We precise that the value of $\alpha(\mathbf{X}, t)$ is not given and (6) could be written without using α by

$$\mathbf{n} \cdot \sigma\left(\mathbf{u}\right)\mathbf{n} \leq 0, \quad \mathbf{t} \cdot \sigma\left(\mathbf{u}\right)\mathbf{n} = 0$$

where $\mathbf{t}$ is the unit tangential vector to $\partial\Omega_0$.

We follow the framework [4], Section 5.3, and (4) means that Γ_C after deformation stays on a given side of ψ_t. Some authors use in place of (4) that the normal displacement is less than a gap function [9], [17] and (4) - (6) are written using complementary unilateral contact boundary conditions.

Now, we introduce the space

$$W = \left\{\mathbf{w} \in \left(H^1\left(\Omega_0\right)\right)^2; \; \mathbf{w} = 0 \text{ on } \Gamma_D\right\},$$

and the bi-linear form $a : W \times W \to \mathbb{R}$,

$$a\left(\mathbf{u}, \mathbf{w}\right) = \int_{\Omega_0} \sigma(\mathbf{u}) : \nabla\mathbf{w} \, d\mathbf{X} = \int_{\Omega_0} \lambda\left(\nabla \cdot \mathbf{u}\right)\left(\nabla \cdot \mathbf{w}\right) + 2\mu\epsilon\left(\mathbf{u}\right) : \epsilon\left(\mathbf{w}\right) \, d\mathbf{X}.$$

The condition (4) can be approached by: $\forall(X_1, X_2) \in \Gamma_C$, $\forall t \in]0, T[$,

$$\psi_t(X_1) + \psi_t'(X_1)\, u_1(X_1, X_2, t) \leq X_2 + u_2(X_1, X_2, t) \tag{9}$$

in the case of linear elasticity, see [7]. For $t \in [0, T]$, the set

$$
\begin{aligned}
K_t \;=\; & \{\mathbf{w} = (w_1, w_2) \in W; \; \forall (X_1, X_2) \in \Gamma_C, \\
& \psi'_t(X_1)\, w_1(X_1, X_2) - w_2(X_1, X_2) \le X_2 - \psi_t(X_1) \}
\end{aligned} \tag{10}
$$

is non empty, closed and convex.

The linear elastodynamics friction-less contact problem can be written formally as a variational inequality: find $\mathbf{u}(t) \in K_t \subset W$, for all $t \in [0, T]$, $\mathbf{u} \in \mathcal{C}^1 \left([0, T]; W\right)$ $\mathbf{u} \in \mathcal{C}^2 \left([0, T]; \left(L^2(\Omega_0)\right)^2\right)$ such that

$$
\rho \int_{\Omega_0} \frac{d^2 \mathbf{u}(t)}{dt^2} \cdot (\mathbf{w} - \mathbf{u}(t))\, d\mathbf{X} + a\left(\mathbf{u}(t), \mathbf{w} - \mathbf{u}(t)\right)
$$

$$
\ge \int_{\Omega_0} \mathbf{f}(t) \cdot (\mathbf{w} - \mathbf{u}(t))\, d\mathbf{X} \; \forall \mathbf{w} \in K_t, \; \forall t \in]0, T[\tag{11}
$$

$$
\mathbf{u}(0) = \mathbf{u}_0 \tag{12}
$$

$$
\frac{d\mathbf{u}}{dt}(0) = \mathbf{u}_1 \tag{13}
$$

with $\mathbf{u}_0 \in K_0$, $\mathbf{u}_1 \in W$, $\mathbf{f} \in \mathcal{C}\left([0, T]; \left(L^2(\Omega_0)\right)^2\right)$. The existence and the regularity of solution for the above problem is open.

3 Mid-point algorithm

We denote by $\Delta t > 0$ the time step, we set $t_n = n\Delta t$, $\mathbf{f}^n = \mathbf{f}(t_n)$ and we denote by $\mathbf{u}^n$, $\mathbf{v}^n$ the approximations of $\mathbf{u}(t_n)$, $\frac{d\mathbf{u}}{dt}(t_n)$, respectively. To simplify, we set $K^n = K_{t_n}$. The mid-point algorithm is: find $\mathbf{u}^{n+1} \in K^{n+1}$ and $\mathbf{v}^{n+1} \in W$ such that

$$
\rho \int_{\Omega_0} \frac{\mathbf{v}^{n+1} - \mathbf{v}^n}{\Delta t} \cdot (\mathbf{w} - \mathbf{u}^{n+1}) d\mathbf{X} + \frac{1}{2} a(\mathbf{u}^{n+1}, \mathbf{w} - \mathbf{u}^{n+1})
$$

$$
+ \; \frac{1}{2} a(\mathbf{u}^n, \mathbf{w} - \mathbf{u}^{n+1}) \ge \int_{\Omega_0} \frac{\mathbf{f}^{n+1} + \mathbf{f}^n}{2} \cdot (\mathbf{w} - \mathbf{u}^{n+1}) d\mathbf{X}, \forall \mathbf{w} \in K^{n+1} \tag{1}
$$

$$
\frac{\mathbf{u}^{n+1} - \mathbf{u}^n}{\Delta t} = \frac{\mathbf{v}^{n+1} + \mathbf{v}^n}{2} \tag{2}
$$

with initial conditions $\mathbf{u}^0 = \mathbf{u}_0$ and $\mathbf{v}^0 = \mathbf{u}_1$.

Proposition 1 *The problem (1) - (2) has a unique solution.*

Proof. From (2), we get $\mathbf{v}^{n+1} = 2\frac{\mathbf{u}^{n+1}-\mathbf{u}^n}{\Delta t} - \mathbf{v}^n$, injected in (1) gives: find $\mathbf{u}^{n+1} \in K^{n+1}$ such that

$$\rho \int_{\Omega_0} 2 \left(\frac{\mathbf{u}^{n+1} - \mathbf{u}^n - \mathbf{v}^n \Delta t}{(\Delta t)^2} \right) \cdot (\mathbf{w} - \mathbf{u}^{n+1}) d\mathbf{X} + \frac{1}{2}a(\mathbf{u}^{n+1}, \mathbf{w} - \mathbf{u}^{n+1})$$

$$\geq -\frac{1}{2}a(\mathbf{u}^n, \mathbf{w} - \mathbf{u}^{n+1}) + \int_{\Omega_0} \frac{\mathbf{f}^{n+1} + \mathbf{f}^n}{2} \cdot (\mathbf{w} - \mathbf{u}^{n+1}) d\mathbf{X}, \forall \mathbf{w} \in K^{n+1}. (3)$$

With the notations $\mathcal{A} : W \times W \to \mathbb{R}$, $L : W \to \mathbb{R}$

$$\mathcal{A}(\mathbf{u}, \mathbf{w}) = \rho \int_{\Omega_0} \frac{2\mathbf{u}}{(\Delta t)^2} \cdot \mathbf{w} d\mathbf{X} + \frac{1}{2}a(\mathbf{u}, \mathbf{w})$$

$$L(\mathbf{w}) = \rho \int_{\Omega_0} \frac{2(\mathbf{u}^n + \mathbf{v}^n \Delta t)}{(\Delta t)^2} \cdot \mathbf{w} \, d\mathbf{X} - \frac{1}{2}a(\mathbf{u}^n, \mathbf{w})$$

$$+ \int_{\Omega_0} \frac{\mathbf{f}^{n+1} + \mathbf{f}^n}{2} \cdot \mathbf{w} \, d\mathbf{X}$$

the problem (3) is equivalent with: find $\mathbf{u}^{n+1} \in K^{n+1}$ such that

$$\mathcal{A}(\mathbf{u}^{n+1}, \mathbf{w} - \mathbf{u}^{n+1}) \geq L(\mathbf{w} - \mathbf{u}^{n+1}), \quad \forall \mathbf{w} \in K^{n+1}. \tag{4}$$

The bilinear function $\mathcal{A}$ is continuous, elliptic, L is continuous and K^{n+1} is non empty, closed, convex, then (4) has a unique solution, see [7]. Then, we put $\mathbf{v}^{n+1} = 2\frac{\mathbf{u}^{n+1}-\mathbf{u}^n}{\Delta t} - \mathbf{v}^n$. We point out that $\mathcal{A}$ is elliptic even when $\Gamma_D = \emptyset$. □

We denote by $\|\mathbf{w}\|_{0,\Omega_0} = \sqrt{\int_{\Omega_0} \mathbf{w} \cdot \mathbf{w} \, d\mathbf{X}}$, the norm of $L^2(\Omega_0)^2$.

Proposition 2 *If $\mathbf{u}^n \in K^{n+1}$ for all $n \in \mathbb{N}$, then there exists a constant $C > 0$ such that*

$$\frac{\rho}{2}\|\mathbf{v}^{n+1}\|^2_{0,\Omega_0} + \frac{1}{2}a(\mathbf{u}^{n+1}, \mathbf{u}^{n+1}) \leq C, \quad \forall n \in \mathbb{N}.$$

Proof. The demonstration is similar to the case without contact. We put in (1), $\mathbf{w} = \mathbf{u}^n$, we get

$$\rho \int_{\Omega_0} \frac{\mathbf{v}^{n+1} - \mathbf{v}^n}{\Delta t} \cdot (\mathbf{u}^{n+1} - \mathbf{u}^n) d\mathbf{X} + \frac{1}{2}a(\mathbf{u}^{n+1} + \mathbf{u}^n, \mathbf{u}^{n+1} - \mathbf{u}^n)$$

$$\leq \int_{\Omega_0} \frac{\mathbf{f}^{n+1} + \mathbf{f}^n}{2} \cdot (\mathbf{u}^{n+1} - \mathbf{u}^n) \, d\mathbf{X}.$$

Using (1), we get

$$\rho \int_{\Omega_0} \frac{\mathbf{v}^{n+1} - \mathbf{v}^n}{\Delta t} \cdot (\mathbf{u}^{n+1} - \mathbf{u}^n) d\mathbf{X} = \rho \int_{\Omega_0} (\mathbf{v}^{n+1} - \mathbf{v}^n) \cdot \frac{\mathbf{v}^{n+1} + \mathbf{v}^n}{2} d\mathbf{X}$$

$$= \frac{\rho}{2} \|\mathbf{v}^{n+1}\|^2_{0,\Omega_0} - \frac{\rho}{2} \|\mathbf{v}^n\|^2_{0,\Omega_0}.$$

From the symmetry of a, we obtain

$$\frac{1}{2} a(\mathbf{u}^{n+1} + \mathbf{u}^n, \mathbf{u}^{n+1} - \mathbf{u}^n) = \frac{1}{2} a(\mathbf{u}^{n+1}, \mathbf{u}^{n+1}) - \frac{1}{2} a(\mathbf{u}^n, \mathbf{u}^n)$$

When $\mathbf{f} = 0$, then

$$\frac{\rho}{2} \|\mathbf{v}^{n+1}\|^2_{0,\Omega_0} - \frac{\rho}{2} \|\mathbf{v}^n\|^2_{0,\Omega_0} + \frac{1}{2} a(\mathbf{u}^{n+1}, \mathbf{u}^{n+1}) - \frac{1}{2} a(\mathbf{u}^n, \mathbf{u}^n) \leq 0$$

and consequently

$$\frac{\rho}{2} \|\mathbf{v}^{n+1}\|^2_{0,\Omega_0} + \frac{1}{2} a(\mathbf{u}^{n+1}, \mathbf{u}^{n+1}) \leq \frac{\rho}{2} \|\mathbf{v}^n\|^2_{0,\Omega_0} + \frac{1}{2} a(\mathbf{u}^n, \mathbf{u}^n) \leq \dots$$

$$\leq \frac{\rho}{2} \|\mathbf{v}^0\|^2_{0,\Omega_0} + \frac{1}{2} a(\mathbf{u}^0, \mathbf{u}^0) = C.$$

The case $\mathbf{f} \neq 0$ is treated as in [10], Section 4.4, mid-point algorithm for elastodynamics without contact, applying the discrete Gronwall lemma. □

We discuss now the case of the non-linear elastic body governed by the St Venant-Kirchhoff model. The right Cauchy-Green deformation tensor is $\mathbf{C} = \mathbf{F}^T \mathbf{F}$, the Green-Lagrange strain tensor is $\mathbf{E} = \frac{1}{2}(\mathbf{C} - \mathbf{I})$, where $\mathbf{F} = \mathbf{I} + \nabla \mathbf{u}$ and for the St Venant-Kirchhoff model, the second Piola-Kirchhoff stress tensors is $\mathbf{\Sigma} = \lambda\, tr(\mathbf{E})\mathbf{I} + 2\mu\mathbf{E}$, with $tr(\mathbf{E}) = E_{11} + E_{22}$.

In the linear case, the sum of the two terms containing a in (1) is equal to

$$a\left(\frac{\mathbf{u}^{n+1} + \mathbf{u}^n}{2}, \mathbf{w} - \mathbf{u}^{n+1}\right).$$

We can obtain the non-linear version of the mid-point algorithm, by replacing the above formula with

$$\int_{\Omega_0} \mathbf{F}^{n+1/2} \mathbf{\Sigma}^{n+1/2} : \nabla\left(\mathbf{w} - \mathbf{u}^{n+1}\right) d\mathbf{X}$$

where $\mathbf{F}^{n+1/2} = \frac{\mathbf{F}^{n+1} + \mathbf{F}^n}{2}$ and $\mathbf{\Sigma}^{n+1/2} = \frac{\mathbf{\Sigma}^{n+1} + \mathbf{\Sigma}^n}{2}$. We can adapt to our case the demonstration from [10], Chapter 5, Section 4, obtained whitout

contact. We can prove that

$$\mathbf{F}^{n+1/2}\boldsymbol{\Sigma}^{n+1/2} : \nabla(\mathbf{U}^{n+1} - \mathbf{U}^n) = \mathbf{F}^{n+1/2}\boldsymbol{\Sigma}^{n+1/2} : (\mathbf{F}^{n+1} - \mathbf{F}^n)$$

$$= \boldsymbol{\Sigma}^{n+1/2} : (\mathbf{E}^{n+1} - \mathbf{E}^n) = \frac{1}{2}(\boldsymbol{\Sigma}^{n+1} + \boldsymbol{\Sigma}^n) : (\mathbf{E}^{n+1} - \mathbf{E}^n).$$

Finnaly, it is obtained that

$$\mathbf{F}^{n+1/2}\boldsymbol{\Sigma}^{n+1/2} : \nabla(\mathbf{U}^{n+1} - \mathbf{U}^n) = \frac{1}{2}\boldsymbol{\Sigma}^{n+1} : \mathbf{E}^{n+1} - \frac{1}{2}\boldsymbol{\Sigma}^n : \mathbf{E}^n.$$

The stability for the St Venant-Kirchhoff model with contact can be derived from the case without contact, i.e. the below energy is bounded

$$\frac{\rho}{2}\|\mathbf{v}^n\|_{0,\Omega_0}^2 + \frac{1}{2}\int_{\Omega_0} \boldsymbol{\Sigma}^n : \mathbf{E}^n.$$

Whitout contact and for dead loading, the mid-point algorithm for the St Venant-Kirchhoff model is an exact energy conservation and second order accuracy scheme, see [15].

4   Numerical results

We consider here, the linear elastic case. We use the finite element software FreeFem++, [6].

4.1   Test 1. Multiple impacts of a disk on a fixed foundation

We use the 2D example from [3]. The undeformed elastic body Ω is a disk of radius $R = 20$ and center $(0, R)$. We set $\Gamma_D = \emptyset$, $\Gamma_N = \partial\Omega \setminus \overline{\Gamma}_C$ and

$$\Gamma_C = \{(x_1(s), x_2(s)); \ x_1(s) = R\cos(s), \ x_2(s) = R + R\sin(s),$$
$$s \in \left(\frac{7\pi}{6}, \frac{11\pi}{6}\right)\right\}.$$

The physical parameters are: Lamé coefficients $\lambda = 30$, $\mu = 30$, mass density $\rho = 1$, externally applied forces per unit volume $\mathbf{f} = (0, -0.1)$, zero externally applied forces on Γ_N, the lowest point of the disk is at the initial position $(0, 4)$ and the initial velocity of the disk is zero. We study the impacts of the disk in the time interval $t \in [0, T]$ with the final time $T = 120$.

The fixed foundation is the horizontal line at $x_2 = 0$. The mesh has 989 vertices, 1864 triangles, 48 segments on Γ_C, 64 segments on Γ_N and $\mathbb{P}_1$ finite element is used.
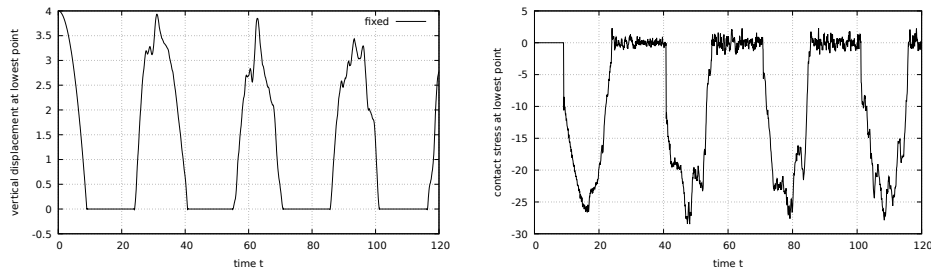
Figure 1: Test 1. Vertical displacement (left) and contact stress (right) at the lowest point.

In [3] the numerical results are obtained by Nitsche, penalty and singular mass methods. Numerical results presented in Figures 1 are similar to the results of [3] obtained by the singular mass method.
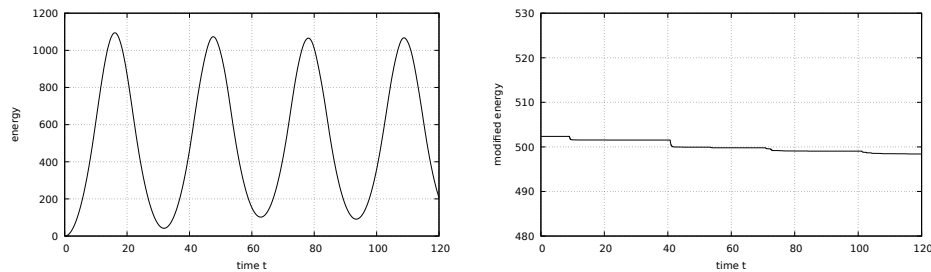

Figure 2: Test 1. Evolution of discrete energy (left) and modified energy (right).

At the first bounce, the body is in contact with the foundation in the time interval $[9, 24]$ and there are no oscillations for the vertical displacement the lowest point of the disk. The oscillations of the contact stress are smaller than for the Nitsche, penalty methods.

We denote by

$$\frac{\rho}{2}\|\mathbf{v}^n\|_{0,\Omega_0}^2 + \frac{1}{2}a(\mathbf{u}^n,\mathbf{u}^n), \quad \frac{\rho}{2}\|\mathbf{v}^n\|_{0,\Omega_0}^2 + \frac{1}{2}a(\mathbf{u}^n,\mathbf{u}^n) - \int_{\Omega_0}\mathbf{f}^n\cdot\mathbf{u}^n d\mathbf{X}$$
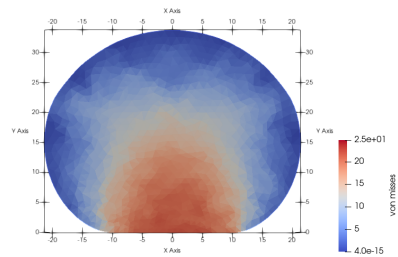
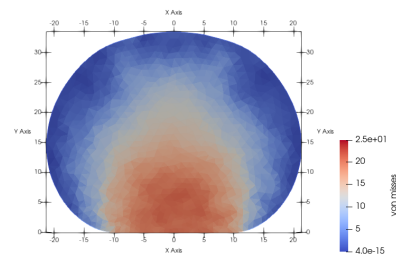the discrete energy and the modified energy, respectively.
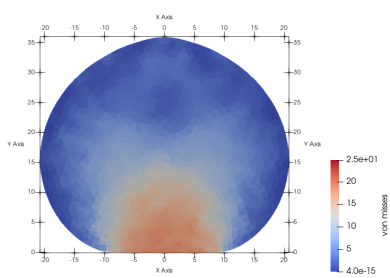
Time: 11.40
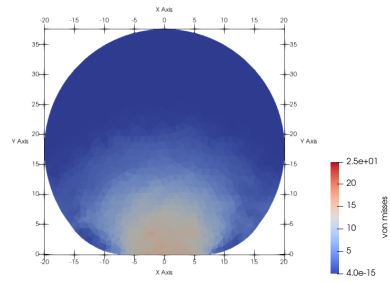
Time: 13.30
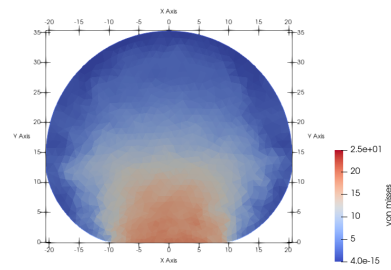
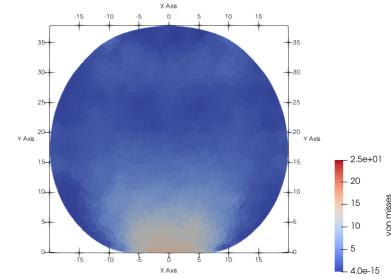Time: 15.25

Time: 17.20

Time: 19.15

Time: 21.10

Figure 3: Test 1. Von Misses stress distribution at the first bounce.

In Figure 2, we observe that the method is a little bit dissipative. For the symmetric stress tensor $\sigma = (\sigma_{ij})_{1 \leq i,j \leq 2}$, the Von Misses stress is given by the formula $(\sigma_{11}^2 - \sigma_{11}\sigma_{22} + \sigma_{22}^2 + 3\sigma_{12}^2)^{1/2}$. The Von Misses stress distributions are presented in Figure 3. We have used the same time instants as in [3].

4.2 Test 2. Multiple impacts of a disk on a moving foundation

We use the disk as in the Test 1, but now the foundation is moving. At each time instant $t \geq 0$, the foundation is the graph of the function $\psi(\cdot, t) : [-30, 30] \to \mathbb{R}$ defined by

$$\psi(X_1, t) = c(t) \cos\left(\frac{\pi}{60} X_1\right) - 2$$

where $c : [0, \infty) \to \mathbb{R}$ is given by

$$c(t) = \begin{cases} 2, & 0 \leq t < t_0, \\ 2\cos\left(\frac{\pi}{2(t_1 - t_0)}\right), & t_0 \leq t < t_1, \\ 0, & t_1 \leq t \end{cases}$$

and $t_0 = 9$, $t_1 = 18$. Initially, the lowest point of the disk is at position $(0, 4)$ and the initial velocity of the disk is zero. We can see the shape of $\psi(\cdot, t)$ before the time instant t_0 in Figure 4. The foundation is decreasing and it is flat after t_1.
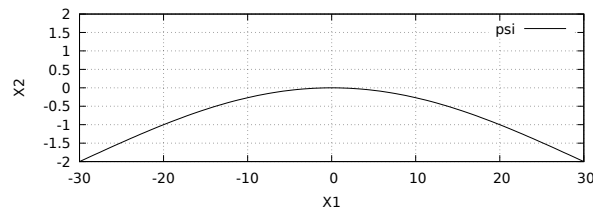

Figure 4: Test 2. Position of $\psi(\cdot, t)$ for $0 \leq t < t_0$. For $t_0 \leq t < t_1$, $\psi(\cdot, t)$ is decreasing and for $t_1 \leq t$, it is the horizontal segment $-30 \leq X_1 \leq 30$, $X_2 = -2$.

In Figure 5, we observe that the vertical displacement is reduced compared to the fixed foundation. Also, for $t_1 = 18$ the reduction is more important than for $t_1 = 22$ or $t_1 = 26$.
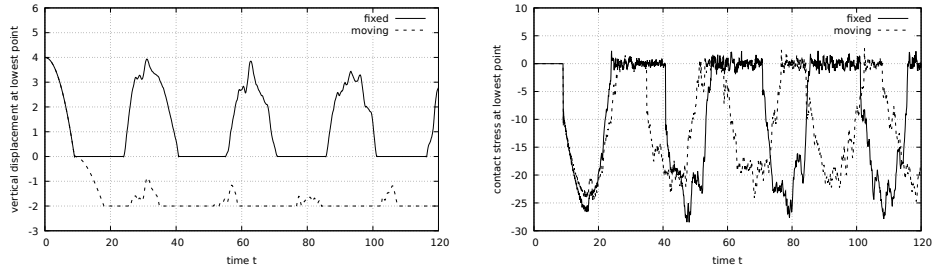
Figure 5: Test 2. Vertical displacement (left) and contact stress (right) at the lowest point.
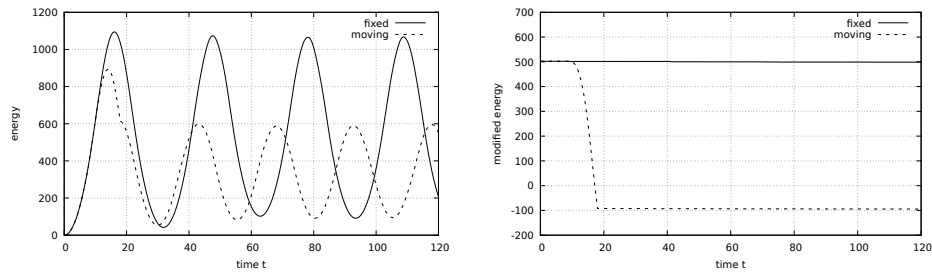

Figure 6: Test 2. Evolution of discrete energy (left) and modified energy (right).

The discrete energy is reduced also, see Figure 6. We observe that the energy is maximal when the body is in contact for the first time with the moving foundation. The modified energy is almost conserved in the case of fixed foundation, but it is absorbed during the decreasing interval $t_0 = 9 \leq t < t_1 = 18$, in the case of moving foundation.
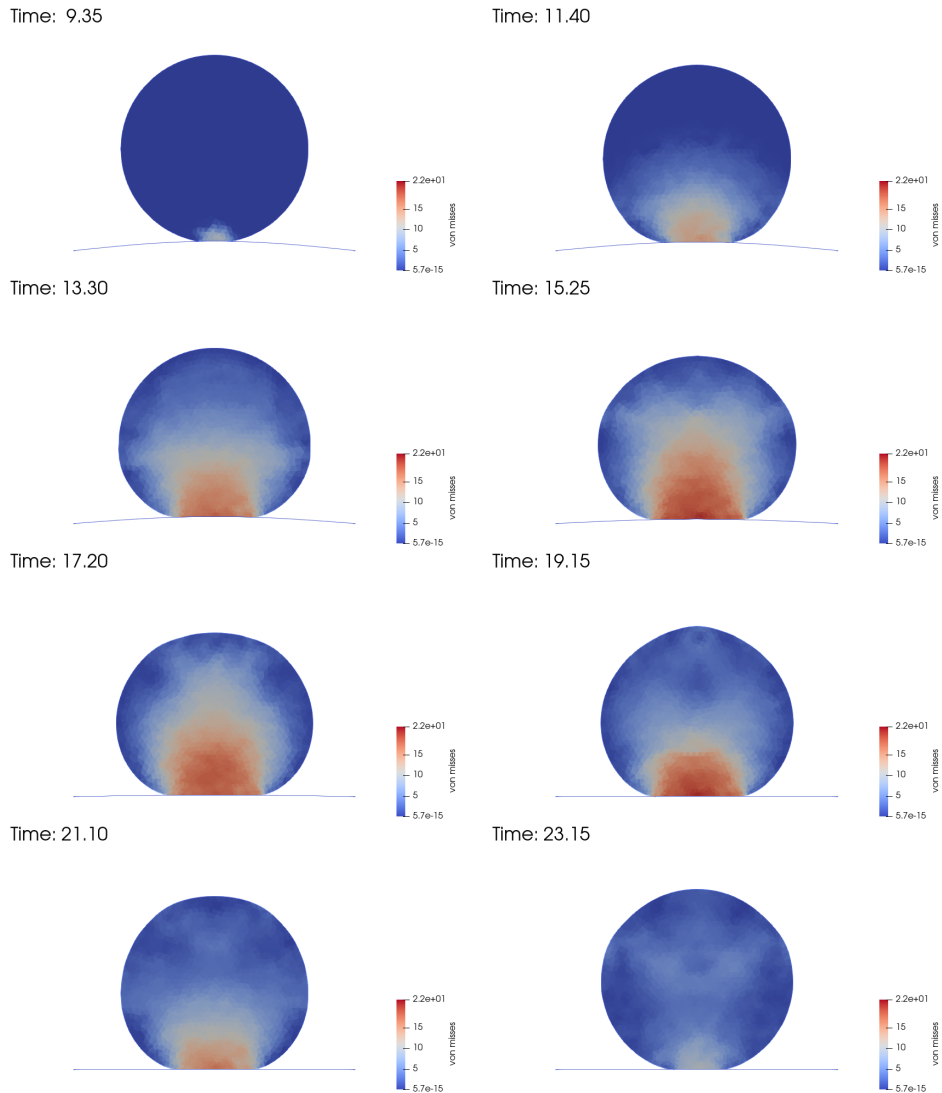
Time: 9.35

Time: 11.40

Time: 13.30

Time: 15.25

Time: 17.20

Time: 19.15

Time: 21.10

Time: 23.15

Figure 7: Test 2. Von Misses stress distribution at the first bounce.

Acknowledgement

References

[1] F. Chouly, P. Hild, Y. Renard, A Nitsche finite element method for dynamic contact: 1. Space semi-discretization and time-marching schemes. *ESAIM Math. Model. Numer. Anal.* 49:481-502, 2015.

[2] F. Chouly, P. Hild, Y. Renard, A Nitsche finite element method for dynamic contact: 2. Stability of the schemes and numerical experiments. *ESAIM Math. Model. Numer. Anal.* 49:503-528, 2015.

[3] F. Chouly, Y. Renard, Explicit Verlet time-integration for a Nitschebased approximation of elastodynamic contact problems. *Advanced Modeling and Simulation in Engineering Sciences,* 5, paper 31, 2018.

[4] P.G. Ciarlet, *Mathematical Elasticity. Volume 1: Three Dimensional Elasticity*, Elsevier, 2004.

[5] D. Doyen, A. Ern, S. Piperno, Time-integration schemes for the finite element dynamic Signorini problem. *SIAM Journal on Scientific Computing*, 33:223-249, 2011.

[6] F. Hecht, New development in FreeFem++. J. Numer. Math. 20 (2012) 251–265. `http://www.freefem.org`

[7] N. Kikuchi, J.T. Oden, *Contact problems in elasticity: a study of variational inequalities and finite element methods.* SIAM Studies in Applied Mathematics, 8. Society for Industrial and Applied Mathematics (SIAM), Philadelphia, 1988.

[8] R. Krause, M. Walloth, Presentation and comparison of selected algorithms for dynamic contact based on the Newmark scheme. *Applied Numerical Mathematics*, 62:1393-1410, 2012.

[9] T.A. Laursen, *Computational contact and impact mechanics. Fundamentals of modeling interfacial phenomena in nonlinear finite element analysis.* Springer Verlag, Berlin, 2002.

[10] C.M. Murea, *Stable Numerical Schemes for Fluids, Structures and their Interactions,* ISTE Press and Elsevier, 2017.

[11] C.M. Murea, Updated Lagrangian for compressible hyperelastic material with frictionless contact, *Appl. Mech.* 3:533-543, 2022.

[12] C.M. Murea, D. Tiba, A direct algorithm in free boundary problems, *J. Numer. Math.*, 24:253-271, 2016.

[13] C.M. Murea, D. Tiba, Approximation of a simply supported plate with obstacle, *Mathematics and Mechanics of Solids*, 23:348-358, 2018.

[14] P. Neittaanmaki, D. Tiba, *Optimal control of nonlinear parabolic systems: theory, algorithms, and applications.* Marcel Dekker, New York, 1994.

[15] J.C. Simo, N. Tarnow, The discrete energy-momentum method. Conserving algorithms for nonlinear elastodynamics, *Zeitschrift fur angewandte Mathematik und Physik ZAMP*, 43:757-792, 1992.

[16] D. Tiba, *Optimal Control of Nonsmooth Distributed Parameter Systems*, Lecture Notes in Mathematics, volume 1459, Springer Berlin, Heidelberg, 1990.

[17] P. Wriggers, *Computational Contact Mechanics.* Springer-Verlag, Berlin, 2006.

[18] O. Yakhlef, C.M. Murea, Numerical simulation of dynamic fluid-structure interaction with elastic structure-rigid obstacle contact, *Fluids*, 6, paper 51, 2021.